

**Single-photon scattering on a qubit: Space-time structure of the scattered field**Ya. S. Greenberg <sup>\*</sup>, A. G. Moiseev, and A. A. Shtygashev*Novosibirsk State Technical University, Department of Radio Engineering and Electronics, 630073, Novosibirsk, Russia*

(Received 6 May 2022; accepted 5 January 2023; published 24 January 2023)

We study the space-time structure of the scattered field induced by the scattering of a narrow single-photon Gaussian pulse on a qubit embedded in a one-dimensional open waveguide. For weak excitation power we obtain explicit analytical expressions for the space and time dependence of reflected and transmitted fields which are, in general, different from plane traveling waves. The scattered field consists of two parts: a damping part which represents spontaneous decay of the excited qubit and a coherent, lossless part. We show that for a large distance  $x$  from the qubit and at times  $t$  long after the scattering event our theory provides the result which is well known from stationary photon transport. However, the approach to the stationary limit is very slow. The scattered field decreases as the inverse powers of  $x$  and  $t$  as both the distance from the qubit and the time after the interaction increase.

DOI: [10.1103/PhysRevA.107.013519](https://doi.org/10.1103/PhysRevA.107.013519)**I. INTRODUCTION**

Manipulating the propagation of photons in a one-dimensional (1D) waveguide coupled to an array of two-level atoms (qubits) may have important applications in quantum devices and quantum information technologies [1–3].

A single photon scattered by a single atom embedded in a 1D open waveguide was first considered in [4,5], where the authors employed the real 1D space description of the Dicke Hamiltonian and the Bethe-ansatz approach [6] to derive the stationary solution for photon transport. It was found that a photon with a frequency equal to that of the two-level atom can be completely reflected due to quantum interference. This property has been experimentally confirmed in the scattering of a microwave photon by a superconducting qubit [7–9].

Since then, theoretical calculations of stationary photon transport in a 1D open waveguide with the atoms placed inside have been performed in a configuration space [10–13] or by alternative methods such as those based on Lippmann-Schwinger scattering theory [14–16], the input-output formalism [17–19], the non-Hermitian Hamiltonian [20], and matrix methods [21,22].

Even though the stationary theory of photon transport provides a useful guide to what one would expect in real experiments, it does not allow for a description of the dynamics of qubit excitation and the evolution of a single-photon pulse.

Within the framework of stationary scattering theories there are only incident and reflected plane waves in front of the qubit and the transmitted plane wave behind the qubit. The reflected and transmitted amplitudes should be understood as the limits of time-dependent description when both the time after the scattering event and the distance from the qubit tend to infinity. Within this approach, all information about the temporal and spatial evolution of the field scattered by the qubit is completely lost. To obtain this information, it is

necessary to consider a time-dependent problem, in which the incident wave is a wave packet that depends on time and coordinates.

In practice, the qubits are excited by photon pulses with finite duration and finite bandwidth. Therefore, to study the real-time evolution of the photon transport and atomic excitation time-dependent dynamical theories were developed [23–27]. In these works, the dynamics of the amplitudes of the qubit and transmitted and reflected waves were considered with an incident single-photon Gaussian packet being scattered by the qubit. The most attention was paid to the reflected and transmitted spectra as the time after the scattering event tends to infinity. In this case, the field scattered by the qubit becomes plane waves and asymptotically approaches the stationary results for photon transport.

Even though the time-dependent theory allows us, in principle, to study the real-time evolution of the scattered field, a systematic and exhaustive discussion of this issue is lacking, except for several numerical plots [23,24,28]. The investigation of the electric field induced by the propagation of a single-photon wave packet through a single atom embedded in a 1D waveguide was performed in [29]. However, in that paper the frequency dependence of transmitted and reflected fields was not studied. The most attention was paid to the on-resonance dependence of transmittance and reflectance on the pulse width.

In the real case, the measurements are performed shortly after the qubit excitation. Under these conditions the reflected and transmitted fields are not plane waves. Therefore, from the point of view of device applications, it is very important to study the real-time evolution and space structure of the scattered field.

In the present paper we consider the scattering of a narrow single-photon Gaussian pulse by a two-level artificial atom (qubit) embedded in a 1D open waveguide. We assume that the bandwidth of the pulse is much smaller than that of any other components of the system. This allows us to obtain explicit analytical expressions for the scattered waveguide

<sup>\*</sup>yakovgreenberg@yahoo.com

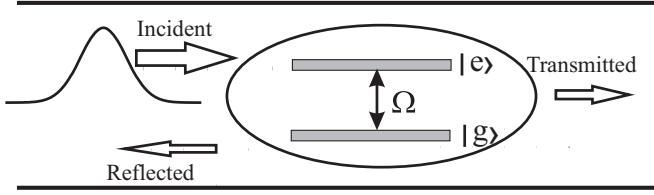


FIG. 1. Schematic representation of a single-photon Gaussian pulse interacting with a two-level atom with energy levels  $|g\rangle$  and  $|e\rangle$ .  $\Omega$  is the separation between the energy levels. Long horizontal lines denote the waveguide geometry.

fields. The scattered fields consist of two parts: a damping part which represents a spontaneous decay of the excited qubit and a coherent, lossless part. We show that for a large distance  $x$  from the qubit and at times  $t$  long after the scattering event our theory for the reflected and transmitted amplitudes provides the result which is well known from stationary scattering theories. However, in general, the structure of the scattered field is different from the stationary limit.

This paper is organized as follows. In Sec. II we introduce the basic parameters describing the transmitted and reflected amplitudes and their asymptotic properties. A general description of our model is given in Sec. III. The interaction between the qubit and electromagnetic field is described by Jaynes-Cummings Hamiltonian. The trial wave function is taken within a single-excitation subspace. From the time-dependent Schrodinger equation we obtain the single-photon amplitudes for forward and backward waves. The main result of this paper is given in Sec. IV. There we construct the photon wave packet for forward- and backward-propagating fields. We obtain explicit expressions for the functions  $F_{T(R)}(\omega_S, x, t)$ , which are given in Eqs. (3) and (4). We show that as both the distance from the qubit and the time after scattering tend to infinity, the stationary results (1) and (2) are recovered. The details of the calculations are given in Appendixes A and B. The influence of the probing power, decoherence rate, and the nonradiative losses on the transmitted and reflected fields is explained in Appendix C.

## II. FORMULATION OF THE PROBLEM

We consider the interaction of a single-photon Gaussian pulse with a two-level atom which is coupled to the waveguide modes with strength  $g$ . The excitation frequency of a qubit is  $\Omega$  (see Fig. 1). A qubit is considered the pointlike emitter, which is placed at the point  $x = 0$  of the  $x$  axis. We assume the interaction of the incident pulse with the qubit starts at  $t = 0$ . It results in reflected and transmitted fields whose space and time structure is the main subject of this paper.

Even though our treatment can be applied to a real two-level atom, we consider here an artificial two-level atom, a superconducting qubit operating at microwave frequencies. For subsequent calculations we take a typical qubit's parameters: the excitation frequency  $\Omega/2\pi = 5$  GHz, which corresponds to the wavelength  $\lambda = 6$  cm, and the rate of spontaneous emission into waveguide modes  $\Gamma/2\pi = 10$  MHz. We assume the group velocity of electromagnetic waves is equal to that of a free space,  $v_g = 3 \times 10^8$  m/s.

The analytical expressions for the transmission  $T$  and reflection  $R$  amplitudes found in the framework of the stationary scattering approach for a monochromatic signal scattered by a two-level atom in a 1D open waveguide [4,5] are as follows:

$$T(\omega_S) = \frac{\omega_S - \Omega}{\omega_S - \Omega + i\frac{\Gamma}{2}}, \quad (1)$$

$$R(\omega_S) = \frac{-i\frac{\Gamma}{2}}{(\omega_S - \Omega + i\frac{\Gamma}{2})}, \quad (2)$$

where  $\omega_S$  is the photon frequency.

It follows from expression (1) that when the photon frequency coincides with the qubit frequency, the value of  $T$  vanishes. In this case, the incident photon is completely reflected from the qubit. The reason for this perfect reflection is coherent interference between the incident wave and the wave scattered by the qubit. It can be said that in this case, the qubit plays the role of an ideal mirror. This behavior was first observed experimentally in the scattering of a microwave photon by a superconducting qubit [7].

Strictly speaking, Eqs. (1) and (2) are valid if we assume a weak probing signal and neglect the qubit's pure dephasing  $\Gamma_\varphi$  and nonradiative intrinsic losses  $\Gamma_l$  [9]. In our treatment below we assume the probe is weak. Under this assumption the pure dephasing and nonradiative losses can simply be incorporated in our treatment by adding the imaginary part to the qubit's frequency  $\Omega$ ,  $\Omega \rightarrow \Omega - i(\Gamma_\varphi + \Gamma_l/2)$ . We address this issue in more detail in Appendix C. It is worth noting that this transformation of qubit frequency gives correct results for transmitted and reflected waves only in the case of single-photon scattering. For few-photon scattering the dephasing and intrinsic losses must be explicitly included in the framework as the Hamiltonian of the external environment from the very beginning [30,31].

From general considerations, it is obvious that the plane-wave solutions (1) and (2) should be a limiting case of a time-dependent picture when both the distance from a qubit and the time after scattering tend to infinity. Near the qubit, the scattered field is more complicated, the amplitude of which depends on the space-time coordinates  $x$  and  $t$  of the scattered field. In the general case, the transmission and reflection fields should have the following form:

$$T(\omega_S, x, t) = T(\omega_S)e^{i\frac{\omega_S}{v_g}(x-v_g t)} + F_T(\omega_S, x, t), \quad (3)$$

$$R(\omega_S, x, t) = R(\omega_S)e^{-i\frac{\omega_S}{v_g}(x+v_g t)} + F_R(\omega_S, x, t). \quad (4)$$

The quantities  $F_{T(R)}(\omega_S, x, t)$  that characterize the space-time structure of the scattered field must satisfy the following property:  $F_{T(R)}(\omega_S, x, t) \rightarrow 0$  at  $|x| \rightarrow \infty$ ,  $t \rightarrow \infty$ . Their structure depends, of course, on the shape of the initial pulse. For a Gaussian wave packet, the structure of  $F_{T(R)}(\omega_S, x, t)$  can be studied only by numerical methods [23,24].

In the present paper, we take the excitation pulse in the form of a Gaussian wave packet which is given by

$$\gamma_0(\omega) = \left(\frac{2}{\pi\Delta^2}\right)^{1/4} e^{-\frac{(\omega-\omega_S)^2}{\Delta^2}}, \quad (5)$$

where  $\omega_S$  is the center frequency of the pulse and  $\Delta$  is the width of the pulse in the frequency domain. We note that the

pulse (5) ensures that there is only a single photon in the wave packet:  $\int_{-\infty}^{\infty} |\gamma_0(\omega)|^2 d\omega = 1$ .

For a narrow pulse we obtain the explicit analytical expressions for the functions  $F_{T(R)}(\omega_S, x, t)$ . These functions decrease relatively slowly (as inverse powers of  $x$  and  $t$ ) for  $x$  and  $t$  that are both large; however, for  $t \rightarrow \infty$  and fixed  $x$ , these functions do not tend to zero. This means that at relatively small distances from the qubit, the field is not uniform, and the dependence of the transmission and reflection amplitudes on the frequency is more complicated than what follows from expressions (1) and (2).

### III. THE MODEL

We consider a single qubit which is located at the point  $x = 0$  in an open linear waveguide. The Hilbert space of the qubit consists of the excited state  $|e\rangle$  and the ground state  $|g\rangle$ . In the continuum limit the Hamiltonian which accounts for the interaction between the qubit and electromagnetic field is as follows [29,32] (we use units where  $\hbar = 1$  throughout the paper):

$$\begin{aligned} H = H_0 &+ \int_0^\infty \omega a^+(\omega) a(\omega) d\omega + \int_0^\infty \omega b^+(\omega) b(\omega) d\omega \\ &+ \int_0^\infty d\omega g(\omega) [\sigma_+ a(\omega) + \sigma_- a^+(\omega)] \\ &+ \int_0^\infty d\omega g(\omega) [\sigma_+ b(\omega) + \sigma_- b^+(\omega)], \end{aligned} \quad (6)$$

where  $H_0$  is the Hamiltonian of the bare qubit,

$$H_0 = \frac{1}{2}(1 + \sigma_z)\Omega. \quad (7)$$

The photon creation and annihilation operators  $a^+(\omega)$  and  $a(\omega)$  and  $b^+(\omega)$  and  $b(\omega)$  describe forward- and backward-scattering waves, respectively. They are independent of each other and satisfy the usual continuous-mode commutation relations [32]:

$$[a(\omega), a^+(\omega')] = \delta(\omega - \omega'); \quad [b(\omega), b^+(\omega')] = \delta(\omega - \omega'). \quad (8)$$

$\sigma_+$  and  $\sigma_-$  are the raising and lowering spin operators, respectively:  $\sigma_+ = |e\rangle\langle g|$  and  $\sigma_- = |g\rangle\langle e|$ . A spin operator  $\sigma_z = |e\rangle\langle e| - |g\rangle\langle g|$ . The quantity  $g(\omega)$  in (6) is the coupling between the qubit and the photon field in a waveguide [29]:

$$g(\omega) = \sqrt{\frac{\omega d^2}{4\pi \epsilon_0 \hbar v_g S}}, \quad (9)$$

where  $d$  is the off-diagonal matrix element of a dipole operator,  $S$  is the effective transverse cross section of the modes in a one-dimensional waveguide, and  $v_g$  is the group velocity of electromagnetic waves. We assume that the coupling is the same for forward and backward waves.

Note that the dimension of the coupling constant  $g(\omega)$  is not the frequency  $\omega$ , but a square root of the frequency,  $\sqrt{\omega}$ , and following (8), the dimension of the creation and destruction operators is  $1/\sqrt{\omega}$ .

Below we consider a single-excitation subspace with either a single photon in the waveguide and the qubit in the ground state or no photons in the waveguide and the qubit being

excited. Therefore, we limit the Hilbert space to the following states:

$$\begin{aligned} |g, 0\rangle &= |g\rangle \otimes |0\rangle, \quad a^+(\omega)|g, 0\rangle = |g\rangle \otimes a^+(\omega)|0\rangle, \\ b^+(\omega)|g, 0\rangle &= |g\rangle \otimes b^+(\omega)|0\rangle. \end{aligned} \quad (10)$$

A trial wave function in the single-excitation subspace reads:

$$\begin{aligned} \Psi(t) &= \beta(t)e^{-i\Omega t}|e, 0\rangle + \int_0^\infty d\omega \gamma(\omega, t)e^{-i\omega t} a^+(\omega)|g, 0\rangle \\ &+ \int_0^\infty d\omega \delta(\omega, t)e^{-i\omega t} b^+(\omega)|g, 0\rangle, \end{aligned} \quad (11)$$

where  $\beta(t)$  is the amplitude of the qubit and  $\gamma(\omega, t)$  and  $\delta(\omega, t)$  are the single-photon amplitudes for forward and backward waves, respectively.

The equations for the quantities  $\beta(t)$ ,  $\gamma(\omega, t)$ , and  $\delta(\omega, t)$  can be found with the time-dependent Schrodinger equation  $id|\Psi\rangle/dt = H|\Psi\rangle$ :

$$\begin{aligned} \frac{d\beta}{dt} &= -i \int_0^\infty d\omega \gamma(\omega, t)g(\omega)e^{-i(\omega-\Omega)t} \\ &- i \int_0^\infty d\omega \delta(\omega, t)g(\omega)e^{-i(\omega-\Omega)t}, \end{aligned} \quad (12)$$

$$\frac{d\gamma(\omega, t)}{dt} = -i\beta(t)g(\omega)e^{i(\omega-\Omega)t}, \quad (13)$$

$$\frac{d\delta(\omega, t)}{dt} = -i\beta(t)g(\omega)e^{i(\omega-\Omega)t}. \quad (14)$$

From Eqs. (13) and (14) we obtain

$$\gamma(\omega, t) = \gamma_0(\omega) - ig(\omega) \int_0^t \beta(t')e^{i(\omega-\Omega)t'} dt', \quad (15)$$

$$\delta(\omega, t) = -ig(\omega) \int_0^t \beta(t')e^{i(\omega-\Omega)t'} dt'. \quad (16)$$

In Eq. (15)  $\gamma_0(\omega) \equiv \gamma(\omega, 0)$  is given in (5).

The substitution of (16) and (15) into Eq. (12) and application of the Wigner-Weisskopf approximation provide the following equation for the qubit amplitude  $\beta(t)$  (the details of the derivation are given in Appendix A):

$$\frac{d\beta}{dt} = -i\sqrt{\frac{\Gamma}{4\pi}} \int_0^\infty \gamma_0(\omega)e^{-i(\omega-\Omega)t} d\omega - \frac{\Gamma}{2}\beta. \quad (17)$$

The integral on the right-hand side of Eq. (17) can be expressed in terms of the error function  $\text{erf}(x)$  [33]:

$$\begin{aligned} \int_0^\infty \gamma_0(\omega)e^{-i(\omega-\Omega)t} d\omega &= \frac{(2\pi)^{1/4}}{2} \sqrt{\Delta} e^{-\frac{\Delta^2 t^2}{4}} \\ &\times \left[ 1 - \text{erf}\left(it\frac{\Delta}{2} - \frac{\omega_S}{\Delta}\right) \right] e^{-i(\omega_S-\Omega)t}. \end{aligned} \quad (18)$$

From now on we consider a narrow pulse where  $\Delta$  is a small quantity, so that  $\Delta \ll \omega_S$ ,  $\Delta t \ll 1$ . In this case  $\text{erf}(it\Delta/2 - \omega_S/\Delta) \approx \text{erf}(-\omega_S/\Delta) \cong -1$ .

Therefore, in the leading order in  $\Delta$  we obtain from (18)

$$\int_0^\infty \gamma_0(\omega)e^{-i(\omega-\Omega)t} d\omega = (2\pi)^{1/4} \sqrt{\Delta} e^{-i(\omega_S-\Omega)t}. \quad (19)$$

Regarding Eq. (19), it is worth noting that in our case a narrow Gaussian pulse can be approximated by a  $\delta$  pulse with the

amplitude  $(2\pi)^{1/4}\sqrt{\Delta}$ :

$$\gamma_0(\omega) = (2\pi)^{1/4}\sqrt{\Delta}\delta(\omega - \omega_s). \quad (20)$$

Finally, Eq. (17) takes the form

$$\frac{d\beta}{dt} = -i(2\pi)^{-1/4}\sqrt{\frac{\Gamma\Delta}{2}}e^{-i(\omega_s-\Omega)t} - \frac{\Gamma}{2}\beta. \quad (21)$$

For an initially unexcited qubit,  $\beta(0) = 0$ , we obtain from (17) the following result for the qubit amplitude:

$$\beta(t) = C_0(e^{-\frac{\Gamma}{2}t} - e^{-i(\omega_s-\Omega)t}), \quad (22)$$

where

$$C_0 = -\frac{(2\pi)^{-1/4}}{\sqrt{2}}\frac{\sqrt{\Gamma\Delta}}{(\omega_s - \Omega + i\frac{\Gamma}{2})}. \quad (23)$$

Finally, for the forward-propagating wave  $\gamma_k(t)$  with  $\beta(t)$  from (22) we obtain

$$\gamma(\omega, t) = \gamma_0(\omega) + \gamma_1(\omega, t), \quad (24)$$

where

$$\gamma_1(\omega, t) = -g(\omega)C_0[I_1(\omega, t) - iI_2(\omega, t)], \quad (25)$$

$$I_1(\omega, t) = \frac{(e^{i(\omega-\Omega+i\frac{\Gamma}{2})t} - 1)}{(\omega - \Omega + i\frac{\Gamma}{2})}, \quad (26)$$

$$I_2(\omega, t) = \int_0^t dt' e^{i(\omega-\omega_s)t'} = \frac{e^{i(\omega-\omega_s)t} - 1}{i(\omega-\omega_s)}. \quad (27)$$

From (15) and (16) we may conclude that the amplitude of the forward-propagating (transmitted) wave is equal to the amplitude of the backward-propagating (reflected) wave,  $\delta(\omega, t) = \gamma_1(\omega, t)$ .

As pointed out in Sec. II and proved in Appendix C, our treatment is valid if we consider a single-photon Gaussian pulse to be a weak excitation probe. For single-photon transport weak excitation means that the pulse duration is much longer than the spontaneous lifetime of the qubit,  $\Delta \ll \Gamma$  [17]. In this case, the qubit is mostly in the ground state. Therefore, we can define the average number of probe photons per interaction time  $2\pi/\Delta$  as  $N = 2\pi P/(\hbar\Omega\Delta)$ , where  $P$  is the power of the incident pulse [8,9]. Taking  $\Delta/2\pi = 1$  MHz and  $\Omega/2\pi = 5$  GHz, we can estimate the power of the incident single-photon Gaussian probe in a weak-excitation limit,  $P \approx \hbar\Omega\Delta/2\pi = 4 \times 10^{-17}$  W. This value is within reach of experimental techniques [8,9].

#### IV. SPACE-TIME STRUCTURE OF THE SCATTERED FIELD

##### A. Forward-scattering field

The photon wave packet for a forward-propagating field behind the qubit is given by

$$\begin{aligned} u(x, t) &= \int_0^\infty d\omega \gamma(\omega, t) e^{i\frac{\omega}{v_g}(x-v_g t)} \\ &= \int_0^\infty d\omega \gamma_0(\omega) e^{i\frac{\omega}{v_g}(x-v_g t)} + \int_0^\infty d\omega \gamma_1(\omega, t) e^{i\frac{\omega}{v_g}(x-v_g t)}, \end{aligned} \quad (28)$$

where  $\gamma_0(\omega)$  is given in (5). In Eqs. (28)  $x > 0$ , and  $x - v_g t < 0$ . The second condition ensures the causality of the propagating field, which does not appear at point  $x$  behind the qubit until the signal travels the distance  $x$  after the scattering.

The first integral on the right-hand side of (28) reads

$$\int_0^\infty d\omega \gamma_0(\omega) e^{i\frac{\omega}{v_g}(x-v_g t)} = (2\pi)^{1/4}\sqrt{\Delta} e^{i\frac{\omega_s}{v_g}(x-v_g t)}, \quad (29)$$

where we use a small  $\Delta$  approximation (20). Therefore, we may consider the prefactor in (29) to be the amplitude of the incoming wave,  $A = (2\pi)^{1/4}\sqrt{\Delta}$ .

For the second integral on the right-hand side of (28) we obtain

$$\begin{aligned} \int_0^\infty d\omega \gamma_1(\omega, t) e^{i\frac{\omega}{v_g}(x-v_g t)} &= -g(\Omega)C_0[I_1(x, t) - iI_2(x, t)] \\ &= A\frac{\Gamma}{4\pi}\frac{1}{\omega_s - \Omega + i\frac{\Gamma}{2}} \\ &\quad \times [I_1(x, t) - iI_2(x, t)], \end{aligned} \quad (30)$$

where

$$I_1(x, t) = \int_0^\infty d\omega I_1(\omega, t) e^{i\frac{\omega}{v_g}(x-v_g t)} d\omega, \quad (31)$$

$$I_2(x, t) = \int_0^\infty d\omega I_2(\omega, t) e^{i\frac{\omega}{v_g}(x-v_g t)} d\omega. \quad (32)$$

In Eq. (30) we use the on-resonance value of the photon-qubit coupling  $g(\Omega)$ ,  $g(\Omega) = \sqrt{\Gamma/4\pi}$  [see the derivation of Eq. (A5) in Appendix A].

The calculations of the quantities  $I_1(x, t)$  and  $I_2(x, t)$  are performed in Appendix B. They are given by

$$\begin{aligned} I_1(x, t) &= e^{-i\tilde{\Omega}t} e^{i\frac{x}{v_g}\tilde{\Omega}} E_1\left(-i\frac{x}{v_g}\tilde{\Omega}\right) + 2\pi i e^{i\frac{\tilde{\Omega}}{v_g}(x-v_g t)} \\ &\quad - e^{-i\frac{|x-v_g t|}{v_g}\tilde{\Omega}} E_1\left(-i\frac{|x-v_g t|}{v_g}\tilde{\Omega}\right), \end{aligned} \quad (33)$$

$$\begin{aligned} I_2(x, t) &= e^{i\frac{\omega_s}{v_g}(x-v_g t)} \left[ 2\pi + i \text{ci}\left(\omega_s \frac{x}{v_g}\right) + \text{si}\left(\omega_s \frac{x}{v_g}\right) \right. \\ &\quad \left. - i \text{ci}\left(\omega_s \frac{|x-v_g t|}{v_g}\right) + \text{si}\left(\omega_s \frac{|x-v_g t|}{v_g}\right) \right], \end{aligned} \quad (34)$$

where  $\tilde{\Omega} = \Omega - i\frac{\Gamma}{2}$ ,  $E_1(z)$  is the exponential integral [34], and  $\text{si}(xy)$  and  $\text{ci}(xy)$  are the sine integral and cosine integral, respectively [33]:

$$\text{ci}(xy) = -\int_x^\infty \frac{\cos zy}{z} dz, \quad \text{si}(xy) = -\int_x^\infty \frac{\sin zy}{z} dz, \quad (35)$$

where  $y$  is  $x/v_g$  or  $|x - v_g t|/v_g$ . In Eqs. (33) and (34)  $x > 0$ , and  $x - v_g t < 0$ .

Combining (29) and (30), we obtain the forward-propagating field behind the qubit in the following form:

$$T(\omega_S, x, t) = T(\omega_S) e^{i\frac{\omega_S}{v_g}(x-v_g t)} + \frac{iR(\omega_S)}{2\pi} e^{i\frac{\Omega}{v_g}(x-v_g t)} e^{\frac{\Gamma/2}{v_g}(x-v_g t)} \left[ E_1\left(i\frac{x}{v_g}\tilde{\Omega}\right) + 2\pi i - E_1\left(-i\frac{|x-v_g t|}{v_g}\tilde{\Omega}\right) \right] + \frac{R(\omega_S)}{2\pi} e^{i\frac{\omega_S}{v_g}(x-v_g t)} \left[ \text{ici}\left(\omega_S\frac{x}{v_g}\right) + \text{si}\left(\omega_S\frac{x}{v_g}\right) - \text{ici}\left(\omega_S\frac{|x-v_g t|}{v_g}\right) + \text{si}\left(\omega_S\frac{|x-v_g t|}{v_g}\right) \right], \quad (36)$$

where  $x > 0$ ,  $x - v_g t < 0$ , and  $T(\omega_S, x, t) \equiv u(x, t)/A$ .

It should be noted that the amplitude of the transmitted field  $T(\omega_S)$  in the first term in (36) is the result of a summation of the incident wave (29) with part of the scattered field [ $2\pi$  in (34)]. The second term in (36) is the damping part of the scattered field which represents spontaneous decay of the excited qubit. The third term in (36) is the coherent, lossless part of the scattered field. As both the distance from the qubit and the time after the scattering tend to infinity, these scattering fields die out, leaving only the plane-wave stationary solution.

Two-dimensional maps of the transmittance  $|T(\omega_S, x, t)|^2$  calculated from (36) for  $t = 1$  ns and  $t = 5$  ns are shown in Fig. 2. In Fig. 2(b) we observe the off-resonance regions around  $\omega_S/\Omega \approx 0.97$  and  $1.03$ , where the transmittance is about 10% larger than 1. This effect persists over the wavelength scale. It can be attributed to the interference between the incident wave and the field generated by the qubit itself. It does not contradict the conception of the probability. In relation to our study the probability is inferred from the conservation of the energy flux: at any instant of time the input energy flux is the sum of the transmitted and reflected energy fluxes integrated over all space and over all frequencies. In our paper we calculate not the energy flux, but the electric field  $u(x, t)$ . Therefore, in this case the conception of the probability is not applicable. As a side comment it is worth noting that a similar amplification of the field exists in Fabry-Pérot interferometers with semitransparent mirrors [35].

### B. Backward-scattering field

The photon wave packet for backward-propagating field before the qubit is as follows:

$$u(x, t) = \int_0^\infty d\omega \delta(\omega, t) e^{-i\frac{\omega}{v_g}(x+v_g t)} = -g(\Omega)C_0[J_1(x, t) - iJ_2(x, t)], \quad (37)$$

where

$$J_1(x, t) = \int_0^\infty I_1(\omega, t) e^{-i\frac{\omega}{v_g}(x+v_g t)} d\omega, \quad (38)$$

$$J_2(x, t) = \int_0^\infty I_2(\omega, t) e^{-i\frac{\omega}{v_g}(x+v_g t)} d\omega. \quad (39)$$

In Eqs. (37), (38), and (39)  $x < 0$ , and  $x + v_g t > 0$ . The second condition ensures the causality of the backscattering field, which does not appear at point  $x$  in front of the qubit until the signal travels the distance  $|x|$  after the scattering.

The quantities  $J_1(x, t)$  and  $J_2(x, t)$  can be calculated similarly to the quantities  $I_1(x, t)$  and  $I_2(x, t)$ . The result is as follows:

$$J_1(x, t) = e^{-i\tilde{\Omega}t} e^{i\frac{|x|}{v_g}\tilde{\Omega}} E_1\left(i\frac{|x|}{v_g}\tilde{\Omega}\right) + 2\pi i e^{-i\frac{\tilde{\Omega}}{v_g}(x+v_g t)} - e^{-i\frac{x+v_g t}{v_g}\tilde{\Omega}} E_1\left(-i\frac{x+v_g t}{v_g}\tilde{\Omega}\right), \quad (40)$$

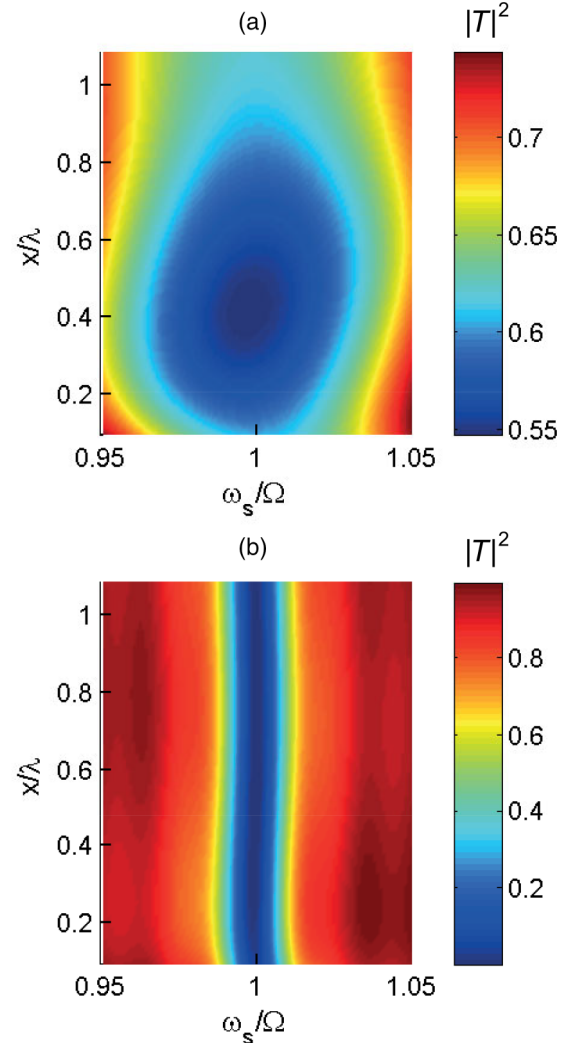


FIG. 2. Two-dimensional map of the transmittance calculated from (36) for (a)  $t = 1$  ns and (b)  $t = 5$  ns. The color bar shows the value  $|T(\omega_S, x, t)|^2$ .  $\Gamma/2\pi = 0.01$  GHz,  $\Omega/2\pi = 5$  GHz, and  $\lambda = 6$  cm.

$$J_2(x, t) = e^{-i\frac{\omega_s}{v_g}(x+v_g t)} \left[ 2\pi + i \operatorname{ci}\left(\omega_s \frac{|x|}{v_g}\right) + \operatorname{si}\left(\omega_s \frac{|x|}{v_g}\right) \right. \\ \left. \times -i \operatorname{ci}\left(\omega_s \frac{x+v_g t}{v_g}\right) + \operatorname{si}\left(\omega_s \frac{x+v_g t}{v_g}\right) \right], \quad (41)$$

where  $x < 0$  and  $x + v_g t > 0$ . Therefore, the backscattered field can be written in the following form:

$$R(\omega_s, x, t) \\ = R(\omega_s) e^{-i\frac{\omega_s}{v_g}(x+v_g t)} + \frac{iR(\omega_s)}{2\pi} e^{-i\frac{\omega_s}{v_g}(x+v_g t)} \\ \times e^{-\frac{\Gamma/2}{v_g}(x+v_g t)} \left[ E_1\left(i\frac{|x|}{v_g}\tilde{\Omega}\right) + 2\pi i - E_1\left(-i\frac{x+v_g t}{v_g}\tilde{\Omega}\right) \right] \\ + \frac{R(\omega_s)}{2\pi} e^{-i\frac{\omega_s}{v_g}(x+v_g t)} \left[ i \operatorname{ci}\left(\omega_s \frac{|x|}{v_g}\right) + \operatorname{si}\left(\omega_s \frac{|x|}{v_g}\right) \right. \\ \left. - i \operatorname{ci}\left(\omega_s \frac{x+v_g t}{v_g}\right) + \operatorname{si}\left(\omega_s \frac{x+v_g t}{v_g}\right) \right], \quad (42)$$

where  $x < 0$ ,  $x + v_g t > 0$ , and  $R(\omega_s, x, t) \equiv u(x, t)/A$ . Here, as in the case of the forward scattering, there are three terms in (42), the stationary solution and damping and coherent parts of the scattered field.

Two-dimensional maps of the reflectance  $|R(\omega_s, x, t)|^2$  calculated from (42) for  $t = 1$  ns and  $t = 5$  ns are shown in Fig. 3.

The first terms in (36) and (42) are just the transmission and reflection amplitudes from the stationary theory. The second lines describe the field generated by spontaneous emission of an excited qubit. This field dies out as the time tends to infinity. The third lines are the transmitted and reflected traveling waves which originate from the interaction of a qubit with the incident photon.

It is worth noting that the scattered fields (36) and (42) display oscillatory behavior in time, as shown in Fig. 4. These oscillations at the frequency  $\omega_s - \Omega$  originate from the interference between the first and second (spontaneous decay) terms in expressions (36) and (42). To avoid the infinity of  $\operatorname{ci}(x\omega_s/v_g)$  at  $x = 0$  we start the calculations in Fig. 4 at  $|x_0| = 1$  mm distance from the qubit and at the time  $t_0 = 10$  ps, which ensures the required condition  $|x_0| - v_g t_0 < 0$ .

A deep analogy exists between the time oscillations of our scattered fields and those of the decay probability in the dynamics of an unstable quantum system [36]. In both cases the time oscillations originate from the effective (after averaging out the photon degrees of freedom) non-Hermitian Hamiltonian.

### C. The scattered field at large time

There are three timescales in our problem:  $1/\Delta$ ,  $1/\Gamma$ , and  $1/\Omega$ , where  $1/\Delta \gg 1/\Gamma \gg 1/\Omega$ . As shown in (19), a weak excitation probe sets the upper bound on the time at which our theory is valid,  $t \ll 1/\Delta$ . Therefore, we may safely satisfy the conditions  $\Gamma t \gg 1$ ,  $\Omega t \gg 1$ , which are necessary to study the asymptotes of the transmitted field (36) and reflected field (42) for a sufficiently large time.

If the time is sufficiently large and  $x$  is fixed, we may disregard the time-dependent corrections in (36) and (42). In

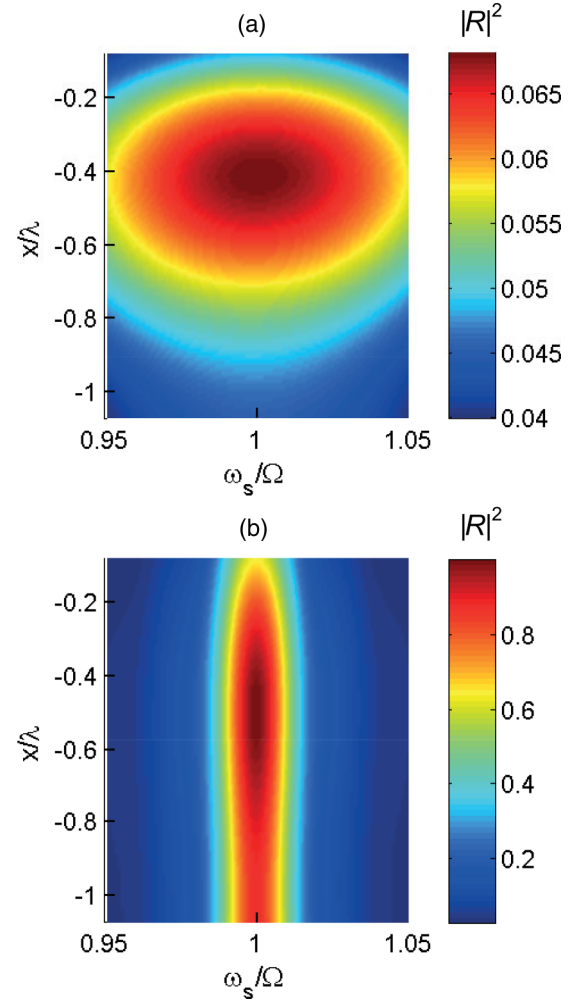


FIG. 3. Two-dimensional map of the reflectance calculated from (42) for (a)  $t = 1$  ns and (b)  $t = 5$  ns. The color bar shows the value  $|R(\omega_s, x, t)|^2$ .  $\Gamma/2\pi = 0.01$  GHz,  $\Omega/2\pi = 5$  GHz, and  $\lambda = 6$  cm.

this case, we obtain from (36) the field behind the qubit:

$$T(\omega_s, x, t) = T(\omega_s) e^{i\frac{\omega_s}{v_g}(x-v_g t)} - \frac{iR(\omega_s)}{2\pi} e^{i\frac{\omega_s}{v_g}(x-v_g t)} \\ \times \left[ i \operatorname{ci}\left(\omega_s \frac{x}{v_g}\right) + \operatorname{si}\left(\omega_s \frac{x}{v_g}\right) \right], \quad (43)$$

where  $T(\omega_s)$  and  $R(\omega_s)$  are transmission and reflection amplitudes (1) and (2), respectively;  $x > 0$ , and  $x - v_g t < 0$ .

From (43) we see that for  $\omega_s = \Omega$  the field at finite distance behind the qubit is nonzero. However, as  $x$  tends to infinity ( $x \gg \lambda$ ), the last term in (43) disappears, and we are left with the stationary transmission amplitude.

Similar calculations from (42) provide the field ahead of the qubit:

$$R(\omega_s, x, t) = R(\omega_s) e^{-i\frac{\omega_s}{v_g}(x+v_g t)} + \frac{R(\omega_s)}{2\pi} e^{-i\frac{\omega_s}{v_g}(x+v_g t)} \\ \times \left[ i \operatorname{ci}\left(\omega_s \frac{|x|}{v_g}\right) + \operatorname{si}\left(\omega_s \frac{|x|}{v_g}\right) \right], \quad (44)$$

where  $R(\omega_s)$  is the reflection amplitude (2);  $x < 0$ , and  $x + v_g t > 0$ . For sufficiently large time the field at a finite distance

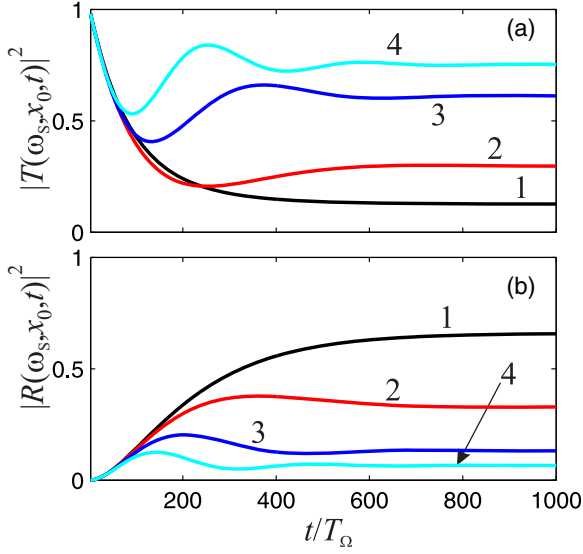


FIG. 4. Dependence of (a) transmittance  $|T(\omega_S, x_0, t \geq t_0)|^2$ , Eq. (36), and (b) reflectance  $|R(\omega_S, x_0, t \geq t_0)|^2$ , Eq. (42) ( $|x_0| = 1$  mm,  $t_0 = 10$  ps), for different frequencies: (1)  $\omega_S = \Omega$ , (2)  $\omega_S = \Omega + 0.5\Gamma$ , (3)  $\omega_S = \Omega + \Gamma$ , and (4)  $\omega_S = \Omega + 1.5\Gamma$ ;  $\Gamma/2\pi = 0.01$  GHz,  $\Omega/2\pi = 5$  GHz, and  $T_\Omega = 2\pi/\Omega$ .

ahead of the qubit remains finite. However, as  $|x|$  tends to infinity ( $|x| \gg \lambda$ ), the last term in (44) disappears, and we are left with the stationary reflection amplitude.

We investigate now how the scattered field [second terms in (43) and (44)] influences the amplitude-frequency curves (AFCs) of transmitted and reflected signals. The dependence of AFCs on the distance from the qubit is shown in Fig. 5.

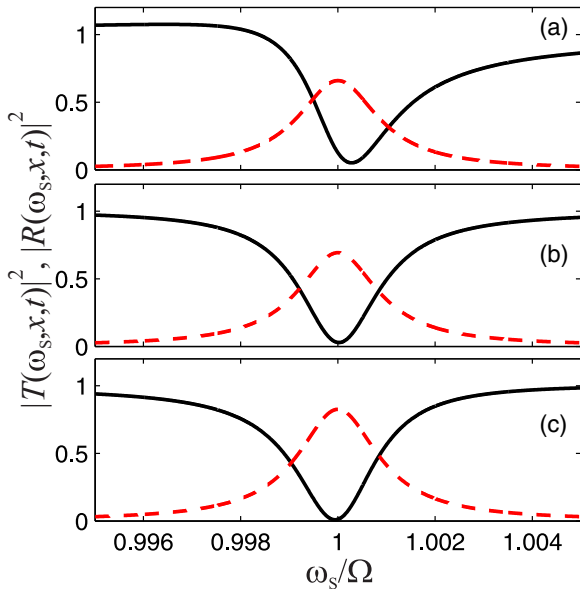


FIG. 5. The dependence of the transmittance (43) (solid black line) and reflectance (44) (dashed red line) on the photon frequency for different distances of the field point from the qubit: (a)  $x = 1$  mm, (b)  $x = 5$  mm, and (c)  $x = 10$  mm.  $\Gamma/2\pi = 0.01$  GHz,  $\Omega/2\pi = 5$  GHz, and  $\lambda = 6$  cm.

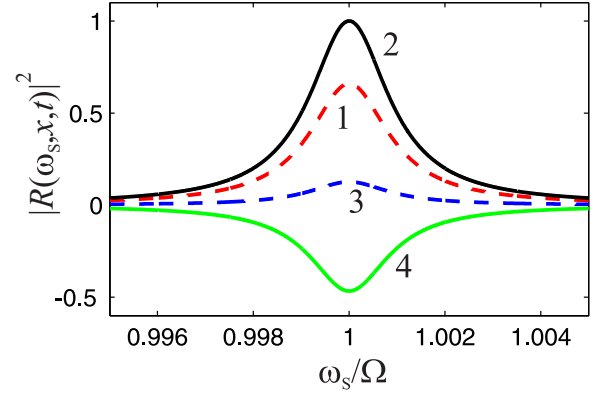


FIG. 6. The influence of the interference on the reflectance (44) at 1-mm distance from the qubit. Dashed red line, labeled 1, the reflectance  $|R(\omega_S, x, t)|^2$ ; solid black line, labeled 2, the reflectance  $|R(\omega_S)|^2$  in the absence of interference; dashed blue line, labeled 3, the term  $|z|^2$ ; solid green line, labeled 4, the interference term  $2|R(\omega_S)|^2\text{Re}(z)$ .  $\Gamma/2\pi = 0.01$  GHz, and  $\Omega/2\pi = 5$  GHz.

We see that a clear asymmetry is observed at  $x = 1$  mm ( $x \ll \lambda$ ) for the transmitted AFC [Fig. 5(a)]. However, for larger  $x$  the asymmetry persists as well. We see in Figs. 5(b) and 5(c) that the transmitted signal at resonance ( $\omega_S = \Omega$ ) is practically zero, while the amplitude of the reflected signal at resonance is appreciably smaller than unity. It can be attributed to the interference between two terms in (44). In fact, from (44) we can write the squared modulus of the reflected field as  $|R(\omega_S, x, t)|^2 = |R(\omega_S)|^2(1 + z)^2$ , where  $z$  is the term in the brackets in (44). The influence of  $z$  on the reflected field at 1-mm distance from the qubit is shown in Fig. 6.

As is seen from Fig. 6, the contribution of the interference term  $2|R(\omega_S)|^2\text{Re}(z)$  is negative (curve 4) and is significant. If the interference term in (44) is neglected, we obtain  $|R(\omega_S)|^2$  for the transmitted signal (curve 2 in Fig. 6).

For off-resonant conditions, the interference effects persist for both reflected and transmitted fields. The influence of these effects on the spatial dependence of the scattered fields is shown in Fig. 7 for  $\omega_S = \Omega, \Omega + 0.5\Gamma, \Omega + \Gamma, \Omega + 1.5\Gamma$ .

From Fig. 7(a) we see that the reflectance at  $x = \lambda/2$  is larger than 1 [see our discussion of Fig. 2(b)]. This amplification can be explained by a constructive interference between incident and reflected waves, as shown in Fig. 8. In this case the interference term  $2|R(\omega_S)|^2\text{Re}(z)$  (line 4 in Fig. 8) is positive (compare it with line 4 in Fig. 6), which gives rise to a small amplification of the reflected field in the resonance region.

In principle, the interference effects can persist over a relatively long distance. As an example we calculate from (43) and (44) the transmittance and reflectance for off-resonant frequency  $\omega_1 = \Omega + 0.5\Gamma$ :

$$|T(\omega_1, x, t)|^2 = \frac{1}{2} \left| 1 - \frac{1}{2\pi} [ici(\alpha) + si(\alpha)] \right|^2, \quad (45)$$

where  $\alpha = \omega_1 x/v_g$ ,  $x > 0$ , and  $x - v_g t < 0$ .

$$|R(\omega_1, x, t)|^2 = \frac{1}{2} \left| 1 + \frac{1}{2\pi} [ici(\alpha) + si(\alpha)] \right|^2, \quad (46)$$

where  $\alpha = \omega_1 |x|/v_g$ ,  $x < 0$ , and  $x + v_g t > 0$ .

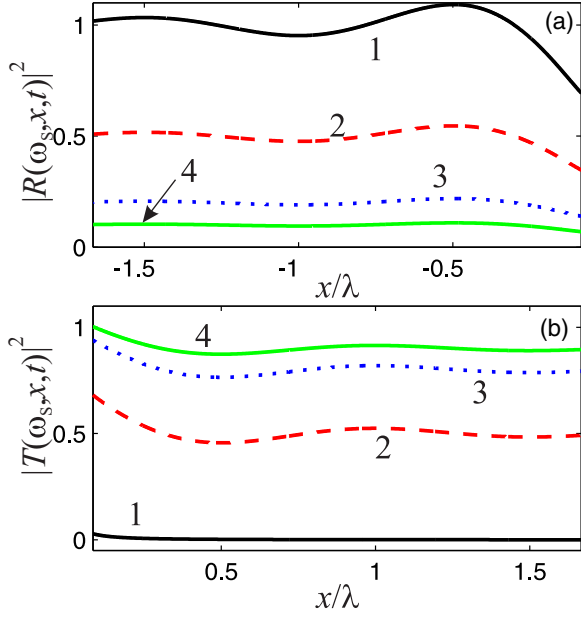


FIG. 7. Spatial dependence of (a) reflectance (44) and (b) transmittance (43) for off-resonant conditions. Solid black line (labeled 1),  $\omega_S = \Omega$ ; dashed red line (labeled 2),  $\omega_S = \Omega + 0.5\Gamma$ ; dotted blue line (labeled 3),  $\omega_S = \Omega + \Gamma$ ; solid green line (labeled 4),  $\omega_S = \Omega + 1.5\Gamma$ .  $\Gamma/2\pi = 0.01$  GHz,  $\Omega/2\pi = 5$  GHz, and  $\lambda = 6$  cm.

The behavior of these quantities at a distance comparable to the photon wavelength follows from the asymptotes of the sine and cosine integrals for large arguments (47). The asymptotic behavior of the interference effects calculated from (45) and (46) is shown in Fig. 9. The envelopes (lines 3 and 4 in Fig. 9) scale as  $\cos(2\pi x/\lambda)/(2\pi x/\lambda)$ .

#### D. Asymptote of the scattered field

The behavior of scattered fields at large  $x$  and  $t$  follows from the asymptote of the exponential integral function, sine

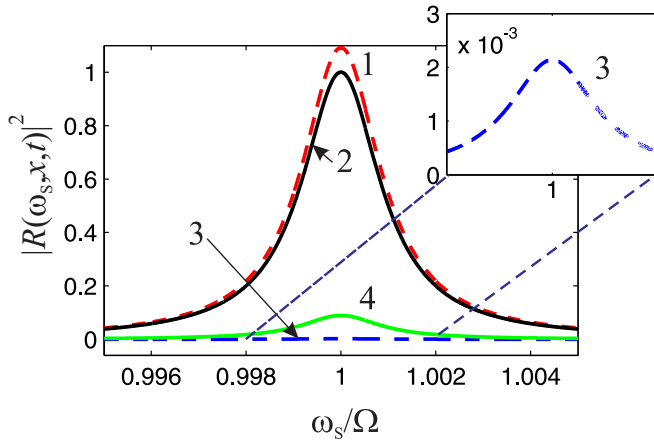


FIG. 8. The influence of the interference on the reflectance (44) at  $x = \lambda/2$  distance from the qubit. Dashed red line (labeled 1), the reflectance  $|R(\omega_S, x, t)|^2$ ; solid black line (labeled 2), the reflectance  $|R(\omega_S)|^2$  in the absence of the interference; dashed blue line (labeled 3), the term  $|z|^2$ ; solid green line (labeled 4), the interference term  $2|R(\omega_S)|^2 \text{Re}(z)$ .  $\Gamma/2\pi = 0.01$  GHz,  $\Omega/2\pi = 5$  GHz, and  $\lambda = 6$  cm.

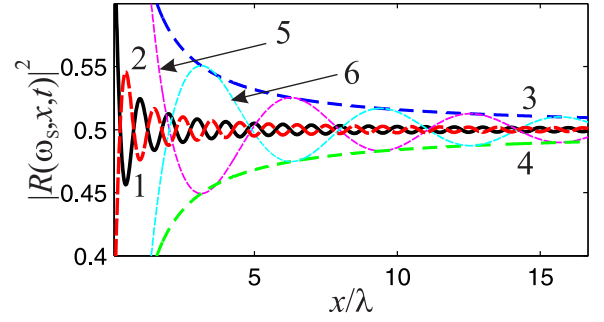


FIG. 9. Spatial dependence of transmittance (solid black line, labeled 1) and reflectance (dashed red line, labeled 2) for the off-resonant condition  $\omega_S = \Omega + 0.5\Gamma$ , calculated from (45) and (46), respectively. The solid magenta line (labeled 5) and solid cyan line (labeled 6) show the asymptotic behavior of transmittance and reflectance, respectively. The dashed blue line (labeled 3) and green line (labeled 4) are the corresponding envelopes.  $\Gamma/2\pi = 0.01$  GHz,  $\Omega/2\pi = 5$  GHz, and  $\lambda = 6$  cm.

integral, and cosine integral [33,37]:

$$\text{si}(x) \approx -\frac{\cos(x)}{x} - \frac{\sin(x)}{x^2}, \quad \text{ci}(x) \approx \frac{\sin(x)}{x} - \frac{\cos(x)}{x^2}, \quad (47)$$

where  $x \gg 1$ .

$$E_1(z) \approx \frac{e^{-z}}{z} \left(1 - \frac{1}{z}\right), \quad (48)$$

where  $|z| \gg 1$ .

With the aid of these approximations we obtain from (36) the asymptotic expression for forward-scattering field:

$$\begin{aligned} T(\omega_S, x, t) &= T(\omega_S) e^{i\frac{\omega_S}{v_g}(x-v_g t)} + \frac{R(\omega_S)}{2\pi} \left( \frac{v_g}{x\tilde{\Omega}} e^{-i(\Omega-i\Gamma/2)t} \right. \\ &\quad \left. - 2\pi e^{i\frac{(\Omega-i\Gamma/2)(x-v_g t)}{v_g}} + \frac{v_g}{|x-v_g t|\tilde{\Omega}} \right) \\ &\quad - \frac{R(\omega_S)}{2\pi} e^{i\frac{\omega_S}{v_g}(x-v_g t)} \left( \frac{v_g}{\omega_S x} e^{-i\frac{\omega_S x}{v_g}} + \frac{v_g}{\omega_S |x-v_g t|} e^{i\frac{\omega_S |x-v_g t|}{v_g}} \right), \end{aligned} \quad (49)$$

where  $x > 0$ ,  $x - v_g t < 0$ ,  $v_g/\omega_S x \ll 1$ ,  $v_g/|x - v_g t|\omega_S \ll 1$ ,  $v_g/\tilde{\Omega}x \ll 1$ , and  $v_g/|x - v_g t|\tilde{\Omega} \ll 1$ . The asymptotic expression for backward-scattering field reads

$$\begin{aligned} R(\omega_S, x, t) &= R(\omega_S) e^{-i\frac{\omega_S}{v_g}(x+v_g t)} + \frac{R(\omega_S)}{2\pi} \left( \frac{v_g}{|x|\tilde{\Omega}} e^{-i(\Omega-i\Gamma/2)t} \right. \\ &\quad \left. - 2\pi e^{-i(\Omega-i\Gamma/2)\frac{(x+v_g t)}{v_g}} + \frac{v_g}{(x+v_g t)\tilde{\Omega}} \right) - \frac{R(\omega_S)}{2\pi} \\ &\quad \times e^{-i\frac{\omega_S}{v_g}(x+v_g t)} \left( e^{-i\omega_S \frac{|x|}{v_g}} \frac{v_g}{\omega_S |x|} + e^{i\omega_S \frac{x+v_g t}{v_g}} \frac{v_g}{\omega_S (x+v_g t)} \right), \end{aligned} \quad (50)$$

where  $x < 0$ ,  $x + v_g t > 0$ ,  $v_g/\omega_S|x| \ll 1$ ,  $v_g/(x + v_g t)\omega_S \ll 1$ ,  $v_g/\tilde{\Omega}|x| \ll 1$ ,  $v_g/|x + v_g t|\tilde{\Omega} \ll 1$ .

We see from (49) and (50) that the approach to the stationary limit is very slow. The scattered field decreases as  $x^{-1}$  and  $t^{-1}$  as the distance from the qubit and the time after the interaction increase.

## V. SUMMARY

In summary, we have developed a time-dependent theory of the scattering of a narrow single-photon Gaussian pulse on a qubit embedded in a 1D open waveguide. For a weak power of the incident pulse we have obtained explicit analytical expressions for the transmitted and reflected fields and their spatial and time dependence. We showed that the scattered field consists of two parts: a damping part which represents spontaneous decay of the excited qubit and a coherent, lossless part. The plane-wave solution for transmission and reflection amplitudes which are well known from the stationary photon transport follows from our theory as the limiting case when both the distance from the qubit and the time after the scattering tend to infinity.

Even though our treatment can be applied to a real two-level atom, we consider in our paper an artificial two-level atom, a superconducting qubit operating at microwave frequencies at gigahertz range. For our calculations we take qubit frequency  $\Omega/2\pi = 5$  GHz, which corresponds to wavelength  $\lambda = 6$  cm. Our calculations showed that spatial effects can persist on the scale of several  $\lambda$  (see Fig. 9). For on-chip realization this length is not small compared with the dimensions of a superconducting qubit (typically several microns). The power of the microwave signal is so low that the use of linear amplifiers for the detection of the qubit signal is a common practice. The current opportunity for on-chip realization of a superconducting qubit with associated circuitry allows for the placement of the amplifier within the order of the wavelength from the qubit. Therefore, in the microwave range the near-field effects can, in principle, be detected.

We believe that the results obtained in this paper may have some practical applications in quantum information technologies, including single-photon detection in a microwave domain as well as the optimization of the readout of a qubit's quantum state.

## ACKNOWLEDGMENTS

Ya.S.G. thanks V. Kurin, who attracted the author's attention to the problem considered in the present paper. This work is supported by the Ministry of Science and Higher Education of the Russian Federation under Project No. FSUN-2023-0006.

### APPENDIX A: DERIVATION OF EQUATION (17)

The substitution of Eqs. (16) and (15) in (12) yields

$$\begin{aligned} \frac{d\beta}{dt} = & -i \int_0^\infty \gamma_0(\omega)g(\omega)e^{-i(\omega-\Omega)t}d\omega - 2 \int_0^\infty d\omega g^2(\omega) \\ & \times \int_0^t \beta(t')e^{-i(\omega-\Omega)(t-t')}dt'. \end{aligned} \quad (\text{A1})$$

The factor of 2 in the last term of (A1) arises from the equal contributions of the forward- and backward-scattering waves to the qubit amplitude  $\beta$ .

In accordance with the Wigner-Weisskopf approximation the quantity  $\beta(t)$  under the integrals in (A1) is assumed to be a slow function of time compared to that of the exponents. Therefore, for times  $\tau = t - t' \ll t$  the integrand oscillates very rapidly, and there is no significant contribution to the value of the integral. The most dominant contribution originates from times  $\tau \approx t$ . We therefore evaluate  $\beta(t)$  at the actual time  $t$  and move it out of the integrand. In this limit, the decay becomes a memoryless process (Markov process):

$$\begin{aligned} \frac{d\beta}{dt} = & -i \int_0^\infty d\omega \gamma_0(\omega)g(\omega)e^{-i(\omega-\Omega)t} - 2\beta(t) \\ & \times \int_0^\infty d\omega g^2(\omega)I(\omega, \Omega, t), \end{aligned} \quad (\text{A2})$$

where

$$I(\omega, \Omega, t) = \int_0^t e^{-i(\omega-\Omega)(t-t')}dt' = \int_0^t e^{-i(\omega-\Omega)\tau}d\tau. \quad (\text{A3})$$

To evaluate this integral we extend the upper integration limit to infinity since there is no significant contribution for  $\tau \gg t$ . Therefore, we obtain

$$I(\omega, \Omega, t) \approx \int_0^\infty e^{-i(\omega-\Omega)\tau}d\tau = \pi\delta(\omega - \Omega) - iP\left(\frac{1}{\omega - \Omega}\right), \quad (\text{A4})$$

where  $P$  represents the Cauchy principal value, which leads to a frequency shift. In what follows, we do not explicitly write this shift, which is assumed to be included in the qubit frequency.

Therefore, Eq. (A2) can be rewritten as follows:

$$\frac{d\beta}{dt} = -i \int_0^\infty d\omega \gamma_0(\omega)g(\omega)e^{-i(\omega-\Omega)t} - \frac{\Gamma}{2}\beta(t), \quad (\text{A5})$$

where  $\Gamma = 4\pi g^2(\Omega)$  is the rate of spontaneous emission into waveguide modes, which also follows from Fermi's golden rule.

The coupling constant  $g(\omega)$  in the first term on the right-hand side of (A5) is a slowly varying function of  $\omega$  around the qubit frequency  $\Omega$ ; therefore, it can be taken out of the integral. Therefore, for Eq. (A5) we finally obtain Eq. (17) from the main text:

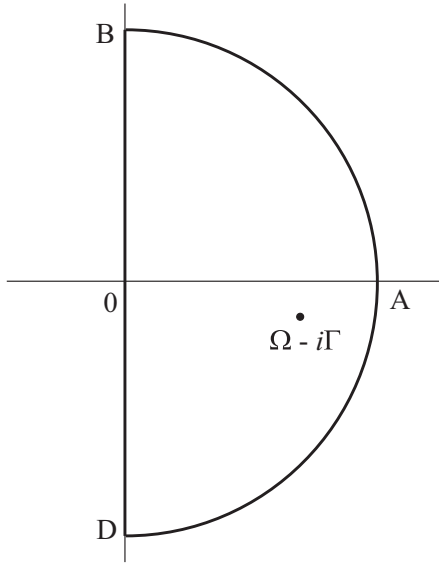
$$\frac{d\beta}{dt} = -i\sqrt{\frac{\Gamma}{4\pi}} \int_0^\infty \gamma_0(\omega)e^{-i(\omega-\Omega)t}d\omega - \frac{\Gamma}{2}\beta(t). \quad (\text{A6})$$

## APPENDIX B: DERIVATION OF EQUATIONS (33) AND (34)

### 1. Calculation of $I_1(x, t)$

The quantity  $I_1(x, t)$  in (31) consists of two terms:  $I_1(x, t) = A(x, t) + B(x, t)$ , where

$$\begin{aligned} A(x, t) = & \int_0^\infty \frac{e^{i(\omega-\tilde{\Omega})t} e^{i\frac{\omega}{v_g}(x-v_g t)}}{(\omega - \tilde{\Omega})}d\omega \\ = & e^{-i\tilde{\Omega}t} \int_0^\infty \frac{e^{i\frac{\omega}{v_g}x}}{(\omega - \tilde{\Omega})}d\omega, \end{aligned} \quad (\text{B1})$$


 FIG. 10. Plane of the complex  $\omega$ .

$$B(x, t) = - \int_0^\infty \frac{e^{i\frac{\omega}{v_g}(x-v_g t)}}{(\omega - \tilde{\Omega})} d\omega. \quad (\text{B2})$$

In the plane of complex  $\omega$  the only pole lies in the lower part of the plane, as shown in Fig. 10. To calculate the last integral in (B1) for  $x > 0$  we take a closed contour  $C_1 = 0AB$ , as shown in Fig. 10. As there are no poles inside this contour, we obtain

$$\oint_{C_1} \frac{e^{i\frac{\omega}{v_g}x}}{(\omega - \tilde{\Omega})} d\omega = 0 = \int_0^\infty \frac{e^{i\frac{\omega}{v_g}x}}{(\omega - \tilde{\Omega})} d\omega + \int_{i\infty}^0 \frac{e^{i\frac{\omega}{v_g}x}}{(\omega - \tilde{\Omega})} d\omega, \quad (\text{B3})$$

$$\int_0^\infty \frac{e^{i\frac{\omega}{v_g}x}}{(\omega - \tilde{\Omega})} d\omega = - \int_{i\infty}^0 \frac{e^{i\frac{\omega}{v_g}x}}{(\omega - \tilde{\Omega})} d\omega = \int_0^{i\infty} \frac{e^{i\frac{\omega}{v_g}x}}{(\omega - \tilde{\Omega})} d\omega. \quad (\text{B4})$$

The last integral in (B4) can be expressed in terms of the exponential integral function  $E_1(z)$  [34]:

$$\int_0^{i\infty} \frac{e^{i\frac{\omega}{v_g}x}}{(\omega - \tilde{\Omega})} d\omega = \int_0^\infty \frac{e^{-\alpha t}}{(t + \beta)} dt = e^{\alpha\beta} E_1(\alpha\beta), \quad (\text{B5})$$

where  $\alpha = x/v_g$ ,  $\beta = i\tilde{\Omega} + \Gamma$ . Therefore, for  $A(x, t)$  we obtain

$$A(x, t) = e^{-i\tilde{\Omega}t} e^{i\frac{x}{v_g}\tilde{\Omega}} E_1\left(i\frac{x}{v_g}\tilde{\Omega}\right), \quad x > 0. \quad (\text{B6})$$

For the calculation of  $B(x, t)$  for  $x - v_g t < 0$  we must take the contour  $C_2 = 0AD$  in the lower part of the complex  $\omega$  plane, as shown in Fig. 10:

$$\begin{aligned} \oint_{C_2} \frac{e^{i\frac{\omega}{v_g}(x-v_g t)}}{(\omega - \tilde{\Omega})} d\omega &= -2\pi i e^{i\frac{\tilde{\Omega}}{v_g}(x-v_g t)} \\ &= \int_0^\infty \frac{e^{i\frac{\omega}{v_g}(x-v_g t)}}{(\omega - \tilde{\Omega})} d\omega + \int_{-i\infty}^0 \frac{e^{i\frac{\omega}{v_g}(x-v_g t)}}{(\omega - \tilde{\Omega})} d\omega. \end{aligned} \quad (\text{B7})$$

From (B7) we obtain

$$\int_0^\infty \frac{e^{i\frac{\omega}{v_g}(x-v_g t)}}{(\omega - \tilde{\Omega})} d\omega = -2\pi i e^{i\frac{\tilde{\Omega}}{v_g}(x-v_g t)} - \int_{-i\infty}^0 \frac{e^{i\frac{\omega}{v_g}(x-v_g t)}}{(\omega - \tilde{\Omega})} d\omega. \quad (\text{B8})$$

The last integral in (B8) can be calculated similarly to (B5):

$$\begin{aligned} \int_{-i\infty}^0 \frac{e^{i\frac{\omega}{v_g}(x-v_g t)}}{(\omega - \tilde{\Omega})} d\omega &= - \int_0^\infty \frac{e^{-\frac{|x-v_g t|s}}{s - i\tilde{\Omega}} ds} \\ &= -e^{-i\frac{|x-v_g t|}{v_g}\tilde{\Omega}} E_1\left(-i\frac{|x-v_g t|}{v_g}\tilde{\Omega}\right). \end{aligned} \quad (\text{B9})$$

Therefore, for  $B(x, t)$  we obtain

$$B(x, t) = 2\pi i e^{i\frac{\tilde{\Omega}}{v_g}(x-v_g t)} - e^{-i\frac{|x-v_g t|}{v_g}\tilde{\Omega}} E_1\left(-i\frac{|x-v_g t|}{v_g}\tilde{\Omega}\right). \quad (\text{B10})$$

Combining (B6) and (B10), we finally obtain

$$\begin{aligned} I_1(x, t) &= e^{-i\tilde{\Omega}t} e^{i\frac{x}{v_g}\tilde{\Omega}} E_1\left(i\frac{x}{v_g}\tilde{\Omega}\right) + 2\pi i e^{i\frac{\tilde{\Omega}}{v_g}(x-v_g t)} \\ &\quad - e^{-i\frac{|x-v_g t|}{v_g}\tilde{\Omega}} E_1\left(-i\frac{|x-v_g t|}{v_g}\tilde{\Omega}\right). \end{aligned} \quad (\text{B11})$$

## 2. Calculation of $I_2(x, t)$

We rewrite (32) as follows:

$$I_2(x, t) = e^{i\frac{\omega_s}{v_g}(x-v_g t)} \frac{1}{i} \int_0^\infty \frac{e^{i(\omega-\omega_s)t} - 1}{(\omega-\omega_s)} e^{i\frac{(\omega-\omega_s)}{v_g}(x-v_g t)} d\omega. \quad (\text{B12})$$

In the integrand of (B12) we introduce the new variables  $\omega - \omega_s = z$  and  $(x - v_g t)/v_g = T$ . We then obtain

$$\begin{aligned} \int_0^\infty \frac{e^{i(\omega-\omega_s)t} - 1}{(\omega-\omega_s)} e^{i\frac{(\omega-\omega_s)}{v_g}(x-v_g t)} d\omega &= \int_{-\omega_s}^\infty \frac{e^{iz\tau}}{z} dz \\ &\quad - \int_{-\omega_s}^\infty \frac{e^{izT}}{z} dz, \end{aligned} \quad (\text{B13})$$

where  $\tau = x/v_g$ .

For the first integral in (B13) we obtain

$$\begin{aligned} \int_{-\omega_s}^\infty \frac{e^{iz\tau}}{z} dz &= \int_{-\omega_s}^\infty \frac{\cos z\tau}{z} dz + i \int_{-\omega_s}^\infty \frac{\sin z\tau}{z} dz \\ &= \int_{-\omega_s}^{\omega_s} \frac{\cos z\tau}{z} dz + \int_{\omega_s}^\infty \frac{\cos z\tau}{z} dz \\ &\quad + i \int_{-\omega_s}^\infty \frac{\sin z\tau}{z} dz \\ &= \int_{\omega_s}^\infty \frac{\cos z\tau}{z} dz + i \int_{-\omega_s}^\infty \frac{\sin z\tau}{z} dz \\ &= -\text{ci}(\omega_s\tau) - i \text{si}(-\omega_s\tau), \end{aligned} \quad (\text{B14})$$

where we introduced the sine and cosine integrals:

$$\text{ci}(\omega_s\tau) = - \int_{\omega_s}^\infty \frac{\cos z\tau}{z} dz, \quad \text{si}(-\omega_s\tau) = - \int_{-\omega_s}^\infty \frac{\sin z\tau}{z} dz. \quad (\text{B15})$$

Similar calculations for the second integral in (B13) yield

$$\int_{-\omega_s}^{\infty} \frac{e^{izT}}{z} dz = -\text{ci}(\omega_s T) - i \text{si}(-\omega_s T), \quad (\text{B16})$$

where

$$\text{ci}(\omega_s T) = -\int_{\omega_s}^{\infty} \frac{\cos zT}{z} dz, \quad \text{si}(-\omega_s T) = -\int_{-\omega_s}^{\infty} \frac{\sin zT}{z} dz. \quad (\text{B17})$$

Finally, we obtain

$$I_2(x, t) = e^{i\frac{\omega_s}{v_g}(x-v_g t)} [i \text{ci}(\omega_s \tau) - \text{si}(-\omega_s \tau) - i \text{ci}(\omega_s T) + \text{si}(-\omega_s T)]. \quad (\text{B18})$$

Next, we use the known property of the sine integral [33],

$$\text{si}(y) + \text{si}(-y) = -\pi, \quad (\text{B19})$$

and two relations which follow from (B17) for  $T < 0$ :

$$\text{si}(-\omega_s T) = -\text{si}(-\omega_s |T|), \quad \text{ci}(\omega_s T) = \text{ci}(\omega_s |T|). \quad (\text{B20})$$

Therefore, for  $I_2(x, t)$  (B18), where  $\tau > 0$  and  $T < 0$ , we finally obtain

$$I_2(x, t) = e^{i\frac{\omega_s}{v_g}(x-v_g t)} [2\pi + i \text{ci}(\omega_s \tau) + \text{si}(\omega_s \tau) - i \text{ci}(\omega_s |T|) + \text{si}(\omega_s |T|)], \quad (\text{B21})$$

which is Eq. (34) from the main text.

### APPENDIX C: THE INFLUENCE OF THE PROBING POWER, DECOHERENCE RATE, AND NONRADIATIVE LOSSES ON THE TRANSMITTED AND REFLECTED FIELDS

By accounting for probing power and all losses, the reflection coefficient can be expressed as [7,9]

$$R(\omega_s) = -\frac{\Gamma}{2\gamma} \frac{1 + i\delta\omega_s/\gamma}{1 + (\delta\omega_s/\gamma)^2 + \Omega_R^2/(\Gamma + \Gamma_l)\gamma}, \quad (\text{C1})$$

where  $\delta\omega_s = \omega_s - \Omega$ ;  $\Omega_R$  is the Rabi oscillation frequency, the square of which is proportional to the power  $P$  of the incident wave; and  $\gamma = \frac{\Gamma}{2} + \Gamma_\varphi + \frac{\Gamma_l}{2}$  is the total decoherence rate, where  $\Gamma_\varphi$  is pure dephasing and  $\Gamma_l$  is the nonradiative intrinsic losses. The transmission coefficient can be found from the relation  $T = 1 + R$ , which holds for a single emitter [7,9]:

$$T(\omega_s) = \frac{1 + (\delta\omega_s/\gamma)^2 - \frac{\Gamma}{2\gamma} [1 + i\delta\omega_s/\gamma] + \frac{\Omega_R^2}{(\Gamma + \Gamma_l)\gamma}}{1 + (\delta\omega_s/\gamma)^2 + \frac{\Omega_R^2}{(\Gamma + \Gamma_l)\gamma}}. \quad (\text{C2})$$

For a probe power in the single-photon regime,  $\Omega_R \ll \Gamma$ , we obtain from (C1) and (C2)

$$R(\omega_s) = \frac{-i\frac{\Gamma}{2}}{\omega - \Omega + i(\frac{\Gamma}{2} + \Gamma_\varphi + \frac{\Gamma_l}{2})}, \quad (\text{C3})$$

$$T(\omega_s) = \frac{\omega - \Omega + i(\Gamma_\varphi + \frac{\Gamma_l}{2})}{\omega - \Omega + i(\frac{\Gamma}{2} + \Gamma_\varphi + \frac{\Gamma_l}{2})}. \quad (\text{C4})$$

Equations (C3) and (C4) coincide with (1) and (2) if we neglect pure dephasing and nonradiative losses. Therefore, as following (C3) and (C4), the pure dephasing and nonradiative losses can be included in the framework of our treatment simply by the redefinition of the qubit's frequency  $\Omega$ ,  $\Omega \rightarrow \Omega - i(\Gamma_\varphi + \Gamma_l/2)$ .

The coupling of the qubit to a waveguide can be described by the relevant quantity  $\beta = \Gamma/2\gamma$ . If we disregard  $\Gamma_\varphi$  and  $\Gamma_l$ , we obtain the critical coupling  $\beta = 1$ , which means that at resonant frequency  $\omega_s = \Omega$  a full extinction of the transmitted signal  $|T(\Omega)|^2 = 0$  and a complete reflection  $|R(\Omega)|^2 = 1$ . However, if we account for dephasing and nonradiative losses, the full extinction of the transmitted field and complete reflection never happen.

- 
- [1] J. M. Raimond, M. Brune, and S. Haroche, Manipulating quantum entanglement with atoms and photons in a cavity, *Rev. Mod. Phys.* **73**, 565 (2001).
- [2] D. Roy, C. M. Wilson, and O. Firstenberg, Strongly interacting photons in one-dimensional continuum, *Rev. Mod. Phys.* **89**, 021001 (2017).
- [3] X. Gu, A. F. Kockum, A. Miranowicz, Y.-X. Liu, and F. Nori, Microwave photonics with superconducting quantum circuits, *Phys. Rep.* **718–719**, 1 (2017).
- [4] J.-T. Shen and S. Fan, Coherent photon transport from spontaneous emission in one-dimensional waveguides, *Opt. Lett.* **30**, 2001 (2005).
- [5] J. T. Shen and S. Fan, Coherent Single Photon Transport in a One-Dimensional Waveguide Coupled with Superconducting Quantum Bits, *Phys. Rev. Lett.* **95**, 213001 (2005).
- [6] V. I. Rupasov and V. I. Yudson, Rigorous theory of cooperative spontaneous emission of radiation from a lumped system of two-level atoms: Bethe ansatz method, *Zh. Eksp. Teor. Fiz.* **87**, 1617 (1984) [*Sov. Phys. JETP* **60**, 927 (1984)].
- [7] O. Astafiev, A. M. Zagoskin, A. A. Abdumalikov, Yu. A. Pashkin, T. Yamamoto, K. Inomata, Y. Nakamura, and J. S. Tsai, Resonance fluorescence of a single artificial atom, *Science* **327**, 840 (2010).
- [8] I.-C. Hoi, C. M. Wilson, G. Johansson, T. Palomaki, B. Peropadre, and P. Delsing, Demonstration of a Single-Photon Router in the Microwave Regime, *Phys. Rev. Lett.* **107**, 073601 (2011).

- [9] I.-C. Hoi, C. M. Wilson, G. Johansson, J. Lindkvist, B. Peropadre, T. Palomaki, and P. Delsing, Microwave quantum optics with an artificial atom in one-dimensional open space, *New J. Phys.* **15**, 025011 (2013).
- [10] J.-T. Shen and S. Fan, Theory of single-photon transport in a single-mode waveguide. I. Coupling to a cavity containing a two-level atom, *Phys. Rev. A* **79**, 023837 (2009).
- [11] M.-T. Cheng, J. Xu, and G. S. Agarwal, Waveguide transport mediated by strong coupling with atoms, *Phys. Rev. A* **95**, 053807 (2017).
- [12] Y.-L. L. Fang, H. Zheng, and H. U. Baranger, One-dimensional waveguide coupled to multiple qubits photon-photon correlations, *EPJ Quantum Technol.* **1**, 3 (2014).
- [13] H. Zheng and H. U. Baranger, Persistent Quantum Beats and Long-Distance Entanglement from Waveguide-Mediated Interactions, *Phys. Rev. Lett.* **110**, 113601 (2013).
- [14] D. Roy, Correlated few-photon transport in one-dimensional waveguides: Linear and nonlinear dispersions, *Phys. Rev. A* **83**, 043823 (2011).
- [15] J.-F. Huang, T. Shi, C. P. Sun, and F. Nori, Controlling single-photon transport in waveguides with finite cross section, *Phys. Rev. A* **88**, 013836 (2013).
- [16] G. Díaz-Camacho, D. Porras, and J. J. Garcia-Ripoll, Photon-mediated qubit interactions in one-dimensional discrete and continuous models, *Phys. Rev. A* **91**, 063828 (2015).
- [17] S. Fan, S. E. Kocabas, and J.-T. Shen, Input-output formalism for few-photon transport in one-dimensional nanophotonic waveguides coupled to a qubit, *Phys. Rev. A* **82**, 063821 (2010).
- [18] K. Lalumiere, B. C. Sanders, A. F. van Loo, A. Fedorov, A. Wallraff, and A. Blais, Input-output theory for waveguide QED with an ensemble of inhomogeneous atoms, *Phys. Rev. A* **88**, 043806 (2013).
- [19] A. H. Kiielerich and K. Molmer, Input-Output Theory with Quantum Pulses, *Phys. Rev. Lett.* **123**, 123604 (2019).
- [20] Ya. S. Greenberg and A. A. Shtygashev, Non-Hermitian Hamiltonian approach to the microwave transmission through a one-dimensional qubit chain, *Phys. Rev. A* **92**, 063835 (2015).
- [21] Ya. S. Greenberg, A. A. Shtygashev, and A. G. Moiseev, Waveguide band-gap  $N$ -qubit array with a tunable transparency resonance, *Phys. Rev. A* **103**, 023508 (2021).
- [22] T. S. Tsoi and C. K. Law, Quantum interference effects of a single photon interacting with an atomic chain, *Phys. Rev. A* **78**, 063832 (2008).
- [23] Y. Chen, M. Wubs, J. Mork, and A. F. Koendrink, Coherent single-photon absorption by single emitters coupled to one-dimensional nanophotonic waveguides, *New J. Phys.* **13**, 103010 (2011).
- [24] Z. Liao, X. Zeng, S.-Y. Zhu, and M. S. Zubairy, Single-photon transport through an atomic chain coupled to a one-dimensional nanophotonic waveguide, *Phys. Rev. A* **92**, 023806 (2015).
- [25] Z. Liao, H. Nha, and M. S. Zubairy, Dynamical theory of single-photon transport in a one-dimensional waveguide coupled to identical and nonidentical emitters, *Phys. Rev. A* **94**, 053842 (2016).
- [26] Z. Liao, X. Zeng, H. Nha, and M. S. Zubairy, Photon transport in a one-dimensional nanophotonic waveguide QED system, *Phys. Scr.* **91**, 063004 (2016).
- [27] C. Zhou, Z. Liao, and M. S. Zubairy, Decay of a single photon in a cavity with atomic mirrors, *Phys. Rev. A* **105**, 033705 (2022).
- [28] G. Drobny, M. Havukainen, and V. Buzek, Stimulated emission via quantum interference Scattering of one-photon packets on an atom in a ground state, *J. Mod. Opt.* **47**, 851 (2000).
- [29] P. Domokos, P. Horak, and H. Ritsch, Quantum description of light-pulse scattering on a single atom in waveguides, *Phys. Rev. A* **65**, 033832 (2002).
- [30] E. Rephaeli and S. Fan, Dissipation in few-photon waveguide transport, *Photonics Res.* **1**, 110 (2013).
- [31] T. Ramos and J. J. Garcia-Ripoll, Correlated dephasing noise in single-photon scattering, *New J. Phys.* **20**, 105007 (2018).
- [32] K. J. Blow, R. Loudon, and S. J. D. Phoenix, Continuum fields in quantum optics, *Phys. Rev. A* **42**, 4102 (1990).
- [33] I. S. Gradshteyn and I. M. Ryzhik, *Table of Integrals, Series, and Products*, 7th ed. (Elsevier, Amsterdam, 2007).
- [34] M. Abramowitz and I. A. Stegun, *Handbook of Mathematical Functions with Formulas, Graphs, and Mathematical Tables* (Dover Publications, Inc., New York, 1965), pp. 228, 5.1.4.
- [35] M. Ley and R. Loudon, Quantum theory of high resolution length measurement with a Fabry Perot interferometer, *J. Mod. Opt.* **34**, 227 (1987).
- [36] M. Peshkin, A. Volya, and V. Zelevinsky, Non-exponential and oscillatory decays in quantum mechanics, *Europhys. Lett.* **107**, 40001 (2014).
- [37] E. Jahnke, F. Emde, and F. Lösch, *Tables of Higher Functions*, 6th ed (McGraw-Hill, New York, 1960).